Journal of Materials Chemistry A

Accepted Manuscript

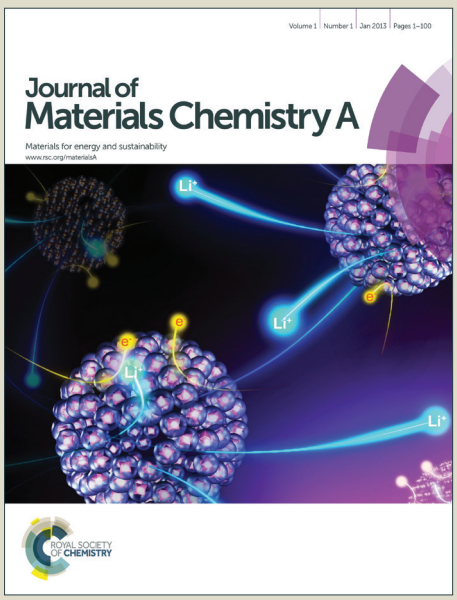

ROYAL SOCIETY OF CHEMISTRY

www.rsc.org/materialsA

Journal Name

RSCPublishing

ARTICLE

Ladder-type Tetra-*p*-phenylene-based Copolymers for Efficient Polymer Solar Cells with Open-circuit Voltages Approaching 1.1 V

Cite this: DOI: 10.1039/x0xx00000x

Received 00th January 2012,
Accepted 00th January 2012

DOI: 10.1039/x0xx00000x

www.rsc.org/

Meng Wang,[ab] Hao Qin,[ab] Lixin Wang,[ab] Jiajun Wei,[ab] Dongdong Cai,[a] Zhigang Yin,[ab] Yunlong Ma,[ab] Shan-Ci Chen,[a] Changquan Tang,[a] and Qingdong Zheng*[a]

Side-chain engineering of the polymer backbone can induce subtle variations in polymer properties, resulting in a significant impact on their photovoltaic performance. In this work, four ladder-type tetra-*p*-phenylene containing copolymers with different alkyl side chains (**P3FTBT1**, **P3FTBT1F**, **P3FTBT8O6** and **P3FTBT1O6**) were designed and synthesized. These copolymers have large bandgaps (~2.0 eV) and deep-lying highest occupied molecular orbital (HOMO) energy levels (from -5.44 eV to -5.53 eV). The substitution of two hexyl groups with two methyl groups on the ladder-type tetra-*p*-phenylene unit afforded polymer **P3FTBT1** which exhibits enhanced power conversion efficiency (PCE) of 5.39%. Incorporation of fluorine into the benzo[c][1,2,5]thiadiazole (**BT)** unit gave polymer **P3FTBT1F** which exhibits a PCE of 4.50% with an open circuit voltage (V_{oc}) of 1.09 V. By introducing two alkoxy groups to the **BT** unit, **P3FTBT1O6** was synthesized, and it exhibits a PCE of 5.73% with a V_{oc} of 1.02 V. The results suggest that the ladder-type tetra-*p*-phenylene is an excellent building block to construct donor-acceptor copolymers with high PCEs and large V_{oc}s.

Introduction

As a new kind of energy conversion devices, solution-processed bulk-heterojunction (BHJ) polymer solar cells (PSCs) have some advantages such as good flexibility, large area processsibility, light weight and low cost, etc.[1-7] Through jointed efforts by many researchers in the organic photovoltaic field, significant breakthroughs have been made in the past decade. At present, both single-junction and tandem PSCs with power conversion efficiencies (PCEs) over 10% have been achieved.[8,9] It is known that in order to get a high PCE PSC, both a large short-circuit current density (J_{sc}) value and a high open-circuit voltage (V_{oc}) are required. So far, an effective strategy to increase the J_{sc} values of PSCs, is to develop low-bandgap conjugated copolymers which can capture more long-wavelength solar light. However, the photovoltaic device based on low-bandgap polymers with a large J_{sc} value often leads to a decreased V_{oc}. As an alternative strategy, researchers have developed tandem devices which stack two or more subcells with complementary absorption spectra. In this way, the V_{oc} of a tandem PSC is close to the sum of the V_{oc}s of the individual cells. Though there have been a large number of low-bandgap polymers for tandem devices, the number of large bandgap (short-wavelength absorbing) copolymers with high PCEs is relatively limited. By now, nearly all tandem solar cells used poly(3-hexylthiophene) (P3HT, 1.90 eV bandgap, HOMO = -5.10 eV) as the short-wavelength absorbing material, which exhibited a low V_{oc} of ~0.70 V (when blended with $PC_{71}BM$). Therefore, in order to enhance the V_{oc}s of tandem solar cells, a replacement of P3HT with spectrally optimized large band-gap polymers is urgently needed.[10-18]

Recently, large or medium band-gap polymers with V_{oc}s exceeding 1.0 V have been developed by a number of research groups.[6,10-16] For example, Lam *et al.* developed a donor-acceptor copolymer using pyrrolo[3,4-f]-2,1,3-benzothiadiazole-5,7-dione as the electron acceptor. Although the resulting PSC exhibited an exceptionally large V_{oc} of 1.10 V, only a low PCE of 1.61 % was achieved due to the low J_{sc} of 4.0 mA/cm^2 and the low FF of 0.33.[12] Casey *et al.* reported a donor-acceptor copolymer (**P2**) using thioalkyl-substituted benzothiadiazole as the electron acceptor. The resulting PSC device exhibited a PCE of 1.92% with a high V_{oc} of 1.07 V.[16] Beaujuge *et al.* developed a medium band-gap (1.79 eV) copolymer based on benzo[1,2-b:4,5-b']dithiophene and thieno [3,4-c]pyrrole-4,6-dione. And the resulting polymer exhibited a high PCE of 6.7% and an outstanding V_{oc} of 1.05 V.[14] In order to have a good current balance for the two individual subcells in tandem devices, the ideal short-wavelength absorbing material should have a large V_{oc}, a high J_{sc} value, and a band-gap as larger as possible. Therefore, large band-gap (>2.0 eV) copolymers with high PCEs and large V_{oc}s will be good candidates as short-wavelength absorbing materials in tandem solar cells.

V_{oc}s of PSCs can be enhanced by tuning the HOMO positions of p-type polymers (donor) and the lowest unoccupied molecular orbital (LUMO) positions of n-type fullerene derivatives (acceptor) to increase the interfacial energy gaps. As fullerene derivatives are the most ubiquitous acceptor molecules employed in PSCs so far, one feasible strategy to enhance the V_{oc}s involves the tuning of HOMO energy positions of p-type conjugated polymers. It has been shown that the combination of a weak donor and a strong

acceptor can lead to copolymers with deep-lying HOMO positions as well as the resulting high V_{oc}s for the devices.[4,12,16] Due to the weak electron donating ability of the fluorene group, many fluorene-based copolymers exhibit deep-lying HOMO energy levels and the resulting high V_{oc}s of the corresponding solar cells.[12] The structure of ladder-type tetra-*p*-phenylene consists of three "linearly overlapping" fluorenes. Compared to fluorene, ladder-type tetra-*p*-phenylene has similar electron donating ability but an extended π-conjugation which may lead to a broader, more intense absorption band of the resulting copolymers. Previously, Zheng *et al.* reported a ladder-type tetra-*p*-phenylene-based D-A copolymer (**P3FTBT6** in Scheme 1**)** with a PCE of 4.5% and a V_{oc} of 1.04 V.[4] However, only a low fill factor of 44% was achieved due to the unoptimized side chains. As it has been disclosed, proper side-chain engineering has an important impact on the polymer properties besides the backbone modification. The side chains of a polymer can affect the molecular weight, solubility, self-assembly, optoelectronic properties and film morphology, which in turn, will affect the performance of the resulting polymer solar cells.[4, 5, 19-22] **BT** is an excellent acceptor unit for D-A copolymers, and therefore it is used to construct the target ladder-type tetra-*p*-phenylene-based copolymers. As usual, two thiophene groups are introduced on the both sides of **BT** group to reduce the steric hindrance between the donor unit and the acceptor unit, which may also affect the properties of the resulting polymer such as carrier mobilities and UV-vis absorption etc.[23-24] For the side-chain engineering of the acceptor unit, three different substituents, i.e, hydrogen, hexyloxy group (electron-donating),[22, 25-28] fluorine atom (electron-withdrawing),[29-35] were introduced. And for the donor unit, we varied the size of the central two alkyl chains on the ladder-type tetra-*p*-phenylene core, from the shortest alkyl group (methyl), to branched alkyl group (ethylhexyl).

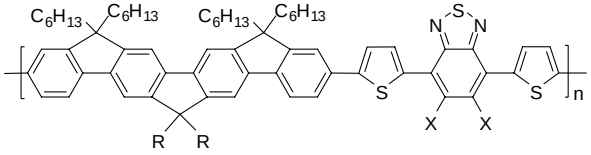

P3FTBT6	R = hexyl	X = H
P3FTBT1	R = methyl	X = H
P3FTBT1F	R = methyl	X = F
P3FTBT8O6	R = 2-ethylhexyl	X = hexyloxy
P3FTBT1O6	R = methyl	X = hexyloxy

Scheme 1 Ladder-type tetra-*p*-phenylene-based copolymers with different side chains.

In this context, we designed and synthesized four D-A copolymers using **BT** as the acceptor unit and ladder-type tetra-*p*-phenylene as the donor unit. The target copolymers (**P3FTBT1**, **P3FTBT1F**, **P3FTBT8O6** and **P3FTBT1O6**) with different side chains either in the donor unit or in the acceptor unit are shown in Scheme 1. The optical, electrochemical and electrical properties of these polymers are investigated together with their photovoltaic performance. Conventional solar cells are fabricated by using the conjugated polymers as donor materials and the $PC_{71}BM$ as the acceptor material. Compared to **P3FTBT6**-based solar cells which showed a maximum PCE of 4.5% and a low FF of 0.42,[4] the best performance device based on **P3FTBT1** exhibits an increased PCE of 5.39% and an improved FF of 51.65%, respectively. The **P3FTBT1F**-based solar cell also exhibits a high V_{oc} of 1.09 V with a PCE of 4.50%. Among all the four copolymers, the best performance device based on **P3FTBT1O6** exhibits the highest PCE of 5.73% with a V_{oc} of 1.02 V.

Experimental

Materials

All Reagents were purchased from commercial sources and used as received without further purification unless otherwise specified. Compounds **1**, **4**, **7**, **8** and **9** were prepared according to the literature procedures.[4, 29, 31, 36-39] The interlayer poly[6,6,12,12-tetra(2-ethylhexyl)-6,12-dihydroindeno[1,2-b]-fluorene-2,8-diyl-alt-2,5-bis(3-(dimethylamino)propoxy) benzene-1,4-diyl] (**PIFB**) was prepared by the copolymerization reaction between 1,4-dibromo-2,5-bis(3-(dimethylamino)propoxy)benzene and 2,2-(6,6,12,12-tetraethylhexyl-6,12-dihydroindeno[1,2b]fluorene-2,8-diyl)bis(4,4,5,5-tetramethyl-1,3,2-dioxaborolane).[40] Column chromatography was conducted with silica gel (300–400 mesh).

Instruments

^1H and ^{13}C NMR spectra were measured on a Bruker AVANCE-400 spectrometer operating at 400 MHz and 100 MHz, respectively. High-resolution mass spectroscopy (HRMS) measurements were performed on an IonSpec 4.7 T spectrometer. Absorption spectra were taken on a spectrophotometer (Lambda 35 UV/vis). Molecular weights and polydispersity indices (PDIs) of the polymers were measured by the gel permeation chromatography (GPC) method in 1,2,4-trichlorobenzene at 150 ^oC (polystyrene as the internal standard). The electrochemical cyclic voltammetry (CV) measurements were performed on a CHI 700E electrochemical workstation. PSCs were measured by a Keithley 2440 source measurement unit under AM 1.5 G irradiation (100 $mW{\cdot}cm^{-2}$) on an Oriel sol3A simulator (Newport) which had been precisely calibrated with a NREL-certified silicon reference cell. The external quantum efficiency (EQE) spectra were performed on a Newport EQE measuring system. The current-voltage curves of organic field effect transistors (OFETs) and hole-only devices were measured by an Agilent 4155C semiconductor parameter analyzer. The thicknesses of polymer films and polymer:$PC_{71}BM$ blended films were measured by the Bruker Dektak XT surface profilometer. Atomic force microscopy (AFM) was performed by the Bruker Dimension FastScan at a tapping mode.

Fabrication of conventional PSCs

The PSCs were fabricated in the traditional single-junction devices with the structure of: indium tin oxide (ITO)/poly(3,4-ethylenedioxythiophene):poly(styrenesulfonate) (PEDOT:PSS)/ polymer:$PC_{71}BM$/PIFB/Al. ITO glass was cleaned by ultrasonication sequentially in detergent, water, acetone, and isopropyl alcohol for 30 min each and then dried in an oven at 90 ^oC overnight. After the ITO glass substrates were subjected to ultraviolet/ozone treatment for 15 min, PEDOT:PSS (Baytron PVPAI 4083) which had been filtered through a 0.45 μm filter was spin-coated on the ITO substrates at 4000 rpm for 60s. Then the film-loaded substrates were dried at 140 ^oC in air for 15 min. Polymers were blended with $PC_{71}BM$ at different weight ratios. The mixtures were dissolved in mixed solvents of chlorobenzene and dichlorobenzene (4/1, v/v) at a concentration of 20 mg/ml and stirred overnight. Then the active layer was prepared by spin-coating the polymer:$PC_{71}BM$ solution at 1500 rpm for 1 min. To facilitate efficient electron injection, a methanol solution of PIFB (0.3 mg/ml containing 30 eq. of acetic acid) was spin-coated to form an electron injection interlayer. Eventually, the negative electrode was prepared by thermally depositing about 100 nm

aluminum through a shadow mask under a high vacuum of about 5 × 10^{-5} Torr. The active areas of the devices were fixed at 4 or 6 mm^2.

Fabrication of FETs and hole-only devices

The heavily doped Si (100) substrates were cleaned by ultrasonication sequentially in piranha solution (H_2SO_4:H_2O_2 = 3:1 by volume), water, acetone, and isopropyl alcohol for 30 min each and then dried in an oven at 90 °C overnight. After the substrates were pretreated with hexamethyldisilazane (HMDS) for 5 hours, the chlorobenzene solution of polymer which had been filtered through a 0.45 μm filter was spin-coated on the substrates at 1500 rpm for 60s. At last, the Au electrode (60 nm) was thermally deposited through a shadow mask to obtain top-contact bottom-gate FETs.

In order to further estimate the hole mobilities of these polymers and polymers:$PC_{71}BM$ blends, we also prepared hole-only devices (ITO/PEDOT:PSS/active layer/MoO_3/Au). The hole-only devices were fabricated following the same procedures as those for the PSCs except that the PIFB layer and Al electrode were replaced by MoO_3 (10 nm) and gold (60 nm), respectively.

Results and discussion

Synthesis and characterization

Compounds **1** and **4** were synthesized according to the literature procedures.[4, 36, 37] As depicted in Scheme 2, compound **1** was treated with n-hexyllithium, ammonium chloride aqueous solution and boron trifluoride etherate successively to get compound **2** in 39% overall yield *via* an intramolecular Friedel-Crafts alkylation. Then, compound **2** was selectively brominated by copper(II) bromide on an alumina matrix in carbon tetrachloride to afford compound **3** in 88% yield. Monomer **6** was synthesized using the same procedures as described above for compound **3**. Monomers **7**, **8** and **9** were prepared according to the procedures reported in the literatures.[29,31, 38,39]

The synthetic route for the copolymers is depicted in Scheme 3. Stille cross-coupling reaction between ladder-type dibromotetra-*p*-phenylene (compound **3** or **6**) and monomer (compound **7**, **8**, or **9**) using $Pd_2(dba)_3$/P(o-tol)$_3$ as the catalytic system afforded D-A copolymers **P3FTBT1**, **P3FTBT1F**, **P3FTBT8O6** and **P3FTBT1O6**. With the help of alkyl chains on the backbone of the polymers, these polymers have good solubility in common organic solvents such as toluene, chloroform, chlorobenzene, etc. GPC results show that the number-average molecular weights (M_n) of **P3FTBT1**, **P3FTBT1F**, **P3FTBT8O6** and **P3FTBT1O6** are 22.0, 14.6, 11.6 and 16.6 kDa, respectively, with the corresponding polydispersity indices (PDIs) of 2.10, 1.75, 1.76 and 2.06, in that order. It should be noted that the incorporating of two F atoms to the **BT** unit leads to bad solubility of the resulting copolymer (**P3FTBT1F**) which in turn leads to its low molecular weight. However, the low molecular weight of **P3FTBT8O6** may be attributed to the more bulky groups in the polymer backbone which prevent the further reaction towards polymers with a larger molecular weight. Thermo gravimetric analysis (TGA) indicates **P3FTBT1**, **P3FTBT1F**, **P3FTBT8O6** and **P3FTBT1O6** are thermally stable with the 5% weight-loss temperature (T_d) values of 430, 430, 336 and 345 °C, respectively (Fig. S1†).

Table 1 Summary of molecular weights, optical and electrochemical properties of the copolymers

Polymers	M_n (kg/mol)	PDI	λ_{max} (nm) in chlorobenzene	λ_{max} (nm) in film	E_g^{opt} (eV)[a]	HOMO (eV)[b]	LUMO (eV)[c]	E_g^{ec} (eV)[d]
P3FTBT1	22.0	2.10	421, 544	419, 552	1.94	-5.44	-3.54	1.90
P3FTBT1F	14.6	1.75	410, 527	404, 528	2.00	-5.51	-3.58	1.93
P3FTBT8O6	11.6	1.76	415, 516	417, 523	2.05	-5.53	-3.56	1.97
P3FTBT1O6	16.6	2.06	423, 522	419, 524	2.04	-5.49	-3.57	1.92

[a]Estimated from the onset of the absorption spectra of thin films. [b]E_{HOMO} = -(φ$_{ox}$+ 4.82) eV, [c]E_{LUMO} = -(φ$_{red}$+ 4.82) eV. [d]E_g^{ec} = electrochemical band-gap (LUMO-HOMO).

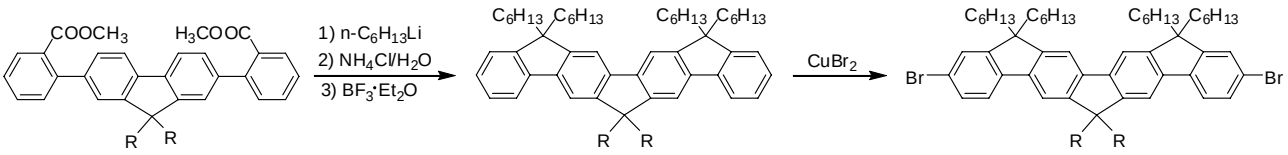

1 R = methyl **2** R = methyl **3** R = methyl

4 R = 2-ethylhexyl **5** R = 2-ethylhexyl **6** R = 2-ethylhexyl

Scheme 2 Synthesis of the monomers **3** and **6**.

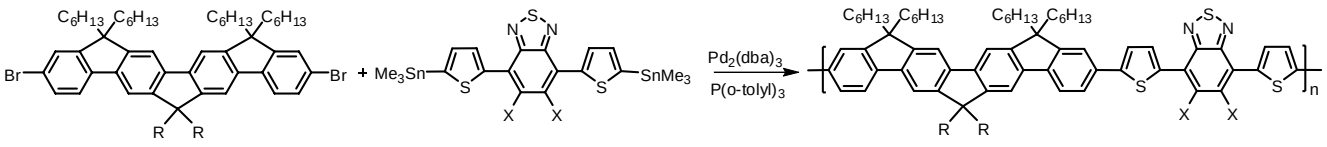

3 R = methyl

6 R = 2-ethylhexyl

7 X = H

8 X = F

9 X = hexyloxy

P3FTBT1 R = methyl X = H

P3FTBT1F R = methyl X = F

P3FTBT8O6 R = 2-ethylhexyl X = hexyloxy

P3FTBT1O6 R = methyl X = hexyloxy

Scheme 3 The synthetic route for the ladder-type tetra-*p*-phenylene containing copolymers.

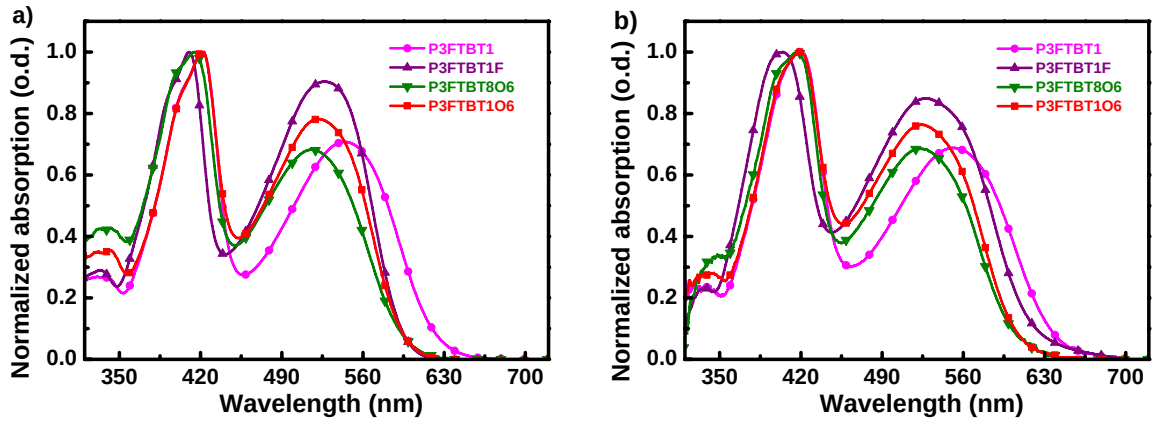

Fig. 1 Normalized UV-vis absorption spectra of the copolymers in 1×10^{-5} M chlorobenzene solution (a) and pure polymer thin film (b).

Optical Properties

The UV-vis absorption spectra of the polymers measured in chlorobenzene solutions (1×10^{-5} M) or in thin films are shown in Fig. 1. Normalized absorption spectra of the copolymers blended with $PC_{71}BM$ are shown in Fig. S2†. The absorption peaks and optical band-gaps of these polymers both in solution and in solid state are also listed in Table 1. All these copolymers have two similar characteristic D-A copolymer absorption bands. The shorter wavelength absorption band is originated from the localized π-π* transition and the longer wavelength absorption peak is due to the intramolecular charge transfer (ICT) from the electron-rich ladder-type tetra-*p*-phenylene part to the electron-deficient **BT** segment. All absorption spectra have similar absorption bandwidth and shape, due to the same main backbone they have. **P3FTBT1** exhibits a low energy absorption maximum at 544 nm in chlorobenzene solution. However, the absorption bands of **P3FTBT1F**, **P3FTBT8O6** and **P3FTBT1O6** shift to 527 nm, 516 nm and 522 nm, respectively. The blue shift absorption bands induced by the incorporation of fluorine or alkoxy group are in agreement with the results found for other copolymers.[40] Compared with their corresponding absorption spectra in solutions, all polymers in thin films show slight bathochromic shift at the longer wavelength. **P3FTBT8O6** with 2-ethylhexyl side chains exhibits blue-shifted absorption in relative to the polymer with methyl side chains (**P3FTBT1O6**) no matter in chlorobenzene or in solid state. This may be due to the branched substituents in the ladder-type tetra-*p*-phenylene skeleton disrupt the planar conformation of the resulting copolymers to some extent. The optical bandgaps (E_g^{opt}) deduced from the onset absorption edges of the polymer films are 1.94, 2.00, 2.05 and 2.04 eV for **P3FTBT1**, **P3FTBT1F**, **P3FTBT8O6** and **P3FTBT1O6**, respectively.

Electrochemical Properties

HOMO and LUMO energy levels of the polymers are crucial for the selection of appropriate acceptor and device structure in BHJ PSCs.[21] The CV measurements were performed by using a three electrode cell system (a Pt disk working electrode coated with polymer chloroform solution to form a thin film, an Ag/Ag^+ (0.1 M $AgNO_3$ in MeCN) reference electrode and a Pt wire counter electrode) in a 0.1 mol/L anhydrous and nitrogen-saturated tetrabutylammonium hexafluorophosphate (Bu_4NPF_6) acetonitrile solution at a scan rate of 100 mV/s. Under this condition, the onset oxidation potential ($E_{1/2\ ox}$) of ferrocene was -0.02 V *versus* Ag/Ag^+. It was assumed that the redox potential of Fc/Fc^+ has an absolute energy level of -4.80 eV to vacuum. The cyclic voltammograms are shown in Fig. 2. The HOMO and LUMO energy levels of the polymers were estimated according to the following equations and summarized in Table 1.

$$E_{HOMO} = -(\varphi_{ox} + 4.82)(eV) \quad (1)$$

$$E_{LUMO} = -(\varphi_{red} + 4.82)(eV) \quad (2)$$

$$E_g^{ec} = (\varphi_{ox} - \varphi_{red})(eV) \quad (3)$$

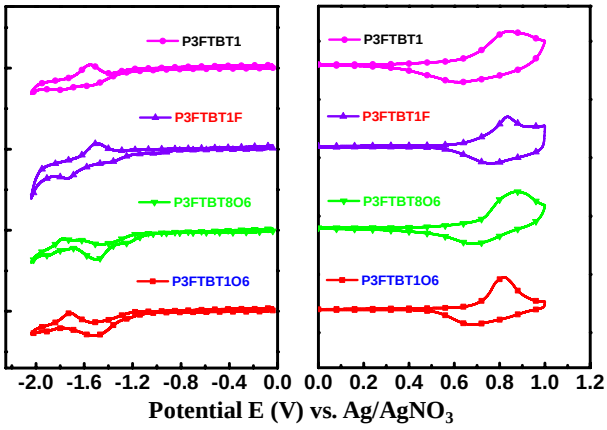

Fig. 2 Cyclic voltammograms of the copolymers.

All the copolymers exhibit oxidation behaviors, indicating these polymers have good stability in the charged state. The HOMO and LUMO energy levels of **P3FTBT1** are located at -5.44 eV and -3.54 eV, respectively. Due to the strong electron-withdrawing property of the F atom, the HOMO and LUMO energy levels of **P3FTBT1F** decrease to -5.51 and -3.58 eV, respectively. After the incorporation of two alkoxy groups, the HOMO energy levels of **P3FTBT8O6** and **P3FTBT1O6** change to -5.53 and -5.49 eV, respectively. All polymers have deep-lying HOMO energy levels and thus they can be used to fabricate PSCs with large V_{oc}s.[41, 42] Larger LUMO offset energy between the polymer and $PC_{71}BM$ benefits the geminate pair dissociation and a higher PCE.[43] The

electrochemical band-gaps of **P3FTBT1**, **P3FTBT1F**, **P3FTBT8O6**, **P3FTBT1O6** are determined to be 1.90, 1.93, 1.97 and 1.92 eV, respectively. The small differences (< 0.13 eV) between electrochemical band-gaps and optical band-gaps for the copolymer are similar to some other amorphous polymers.[28]

Hole Mobilities

The mobilities are important parameters to fabricate high performance PSCs. Because $PC_{71}BM$ has enough high electron transporting ability to afford sufficient electron mobility, the hole mobilities of copolymers are crucial for the PSCs. In this work, we measured hole mobilities of these copolymers by fabricating OFETs and hole-only devices.

Transfer curves of OFETs based on the polymers are shown in Fig. S3†, where I_d represents the source-drain current and V_g represents the source-drain voltage. The mobilities were calculated from the transfer characteristics of the OFETs using the slope derived from the square root of the absolute value of the current as a function of the gate voltage. The hole motilities for **P3FTBT1**, **P3FTBT1F**, **P3FTBT8O6** and **P3FTBT1O6** are $(1.43 \pm 0.07) \times 10^{-3}$, $(2.68 \pm 0.15) \times 10^{-3}$, $(5.48 \pm 0.17) \times 10^{-5}$ and $(2.15 \pm 0.05) \times 10^{-3}$ $cm^2 \cdot V^{-1} \cdot s^{-1}$, respectively. The hole motilities for **P3FTBT1**, **P3FTBT1F** and **P3FTBT1O6** are higher than that for **P3FTBT8O6**. There was a pronounced mobility difference between **P3FTBT1O6** and **P3FTBT8O6**, and the mobility of the former is about 40 times higher than that of the latter, demonstrating the strong effect of alkyl chain on hole transporting property of copolymers. It should be mentioned that the structure difference in **P3FTBT1O6** and **P3FTBT8O6** is the length of central side chains on the donor unit.

The OFETs show hole migration ability in the horizontal direction. As polymers are anisotropy, hole mobilities in horizontal and vertical directions may be different. Therefore, the hole mobilities of the polymers were also estimated with the space charge limited current (SCLC) method and hole-only devices (ITO/PEDOT: PSS/polymer (or polymer:$PC_{71}BM$)/MoO_3/Au). The SCLC hole mobilities were calculated according to the following equation:

$$J = \frac{9}{8}\varepsilon_r \varepsilon_0 \mu \frac{V^2}{L^3} \quad (4)$$

where J is the current, ε_r is the dielectric constant of the polymer (assumed to be 3), ε_0 is the permittivity of free space (8.85×10^{-12} F m^{-1}), μ is the carrier mobility, V is the voltage drop across the device ($V = V_{appl} - V_a - V_{bi}$, where V_{appl} is the applied voltage to the device, V_a is the voltage drop due to contact resistance and series resistance across the electrodes, and V_{bi} is the built-in voltage due to the difference in work function of the two electrodes, and L is the film thickness of polymer or polymer:$PC_{71}BM$ blend. The $J^{0.5}$-V curves are shown in Fig. S4†. The hole mobilities of **P3FTBT1**, **P3FTBT1F**, **P3FTBT8O6** and **P3FTBT1O6** are estimated to be $(8.00 \pm 0.62) \times 10^{-6}$, $(6.92 \pm 0.61) \times 10^{-6}$, $(2.46 \pm 0.24) \times 10^{-6}$ and $(1.24 \pm 0.12) \times 10^{-5}$ $cm^2 \cdot V^{-1} \cdot s^{-1}$, respectively. The hole mobilites measured by OFETs are hundreds times higher than those estimated by the SCLC method similar to the reported finding.[44] **P3FTBT1O6** has the highest μ_{SCLC} value to assure enough charge transport and may lead to PSCs with the highest PCE among these polymers. However, **P3FTBT8O6** has the lowest μ_{SCLC} value due to the bulky 2-ethylhexyl groups in its polymer backbone which may be against a good π-π packing in the solid state.

Photovoltaic Properties

A conventional device architecture of ITO/PEDOT: PSS/polymer:$PC_{71}BM$/PIFB/Al was used to investigate the photovoltaic properties of the polymers. In order to get well balanced electron/ hole mobilities, the donor:acceptor (D:A) ratios of the active layers are optimized toward better device performance. The photovoltaic parameters (V_{oc}, J_{sc}, FF and PCE) are summarized in Table 2 and Tables S1-S3†. As shown in Table 2, and Tables S1-S3†, the optimized weight ratio of polymer to $PC_{71}BM$ is 1:4.5 for all the four copolymers. Here, **P3FTBT1O6** was used as an example to demonstrate the effect of the blend ratio on the performance of solar cells. The J-V curves and the EQE spectra for PSCs based on **P3FTBT1O6**:$PC_{71}BM$ with different blend ratios (D:A = 1:3.0, 1:4.0, 1:4.5 and 1:5.0) are plotted in Fig. 3. And the photovoltaic performance enhancements of **P3FTBT1O6**: $PC_{71}BM$-based devices are shown in Fig. 4. As shown in Fig. 4, the V_{oc} remains almost unchanged with the change in $PC_{71}BM$ content. However, with the increasing $PC_{71}BM$ content, increased FF, J_{sc}, and PCE are observed in the weight ratio between 3.0:1 and 4.5:1. When the blend ratio of $PC_{71}BM$:**P3FTBT1O6** further increases to 5.0:1, decreased FF, J_{sc}, and PCE are observed. This performance dependence trend is also reflected from the corresponding R_s values of the devices as shown in Table 2. It is attributed to the fact that the V_{oc} is mainly depended on the energy levels of the polymer, $PC_{71}BM$, PIFB and PEDOT:PSS. Whereas, J_{sc}, FF, and PCE for the PSCs are closely related with the hole and electron mobilities of the active layers which are strongly influenced by the polymer:$PC_{71}BM$ blend ratio.

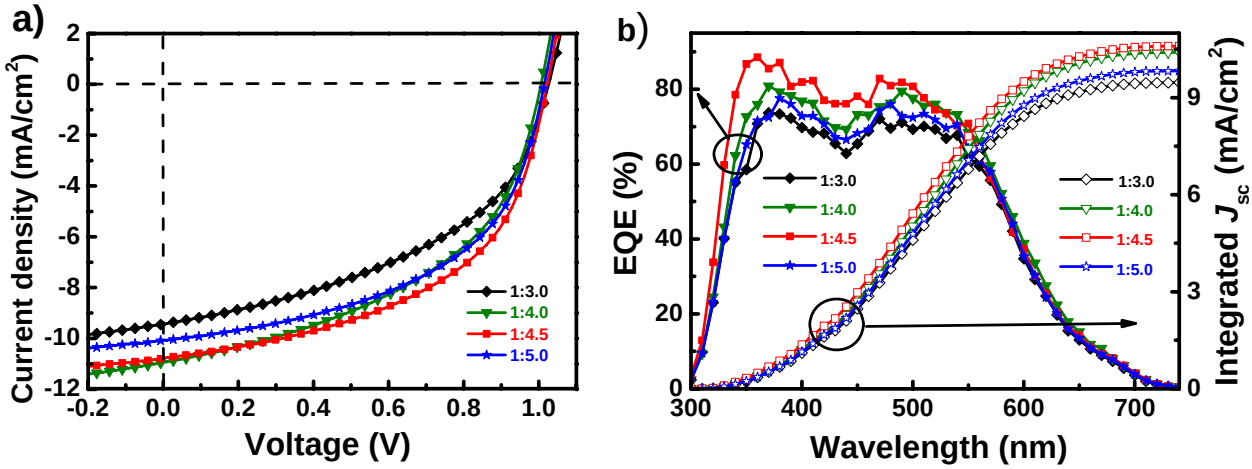

Fig. 3 a) J–V curves and b) EQE and corresponding integrated J_{sc} curves of PSCs based on **P3FTBT1O6** blended with $PC_{71}BM$ with various blend ratios.

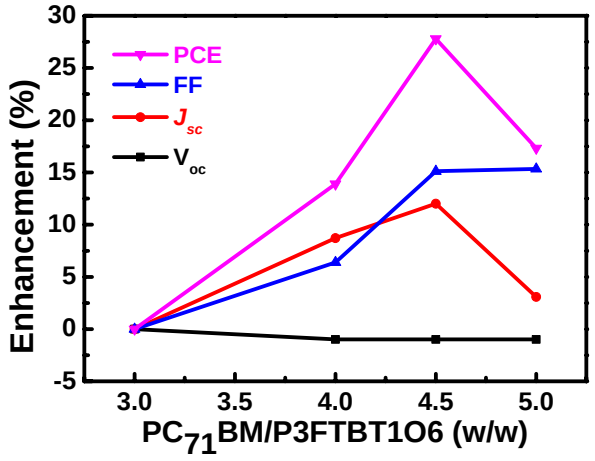

Fig. 4 The average photovoltaic performance enhancements of **P3FTBT1O6**:$PC_{71}BM$-based devices with different blend ratios.

To explain the impacts of blend ratio on the polymer photovoltaic performance, hole mobilities of **P3FTBT1O6**:$PC_{71}BM$ blend films with various blend ratios were investigated by the SCLC method. The dark current density-voltage (J_{dark}-V) characteristics of these hole-only devices are plotted in Fig. S5 † . The hole mobilities of the **P3FTBT1O6**:$PC_{71}BM$ blend films with various blend ratios (D:A = 1:3.0, 1:4.0, 1:4.5 and 1:5.0) are $(1.17 \pm 0.08) \times 10^{-4}$, $(3.73 \pm 0.68) \times 10^{-4}$, $(4.73 \pm 0.57) \times 10^{-4}$ and $(1.25 \pm 0.23) \times 10^{-4}$ $cm^2 \cdot V^{-1} \cdot s^{-1}$, respectively. When the blend ratio of **P3FTBT1O6**:$PC_{71}BM$ decreases from 1:3, to 1:4, and to 1:4.5, the hole mobilities of the blends increase monotonously. A further decreased blend ratio to 1:5.0 leads to decreased hole mobilities. These results are in agreement with the J_{sc} and PCE changes for the PSCs based on **P3FTBT1O6**. When the **P3FTBT1O6**:$PC_{71}BM$ blend ratio is 1:4.5, the active layer may have more balanced hole and electron mobilities which contribute to the high J_{sc}, FF and PCE. As a result, solar cells fabricated from **P3FTBT1O6**:$PC_{71}BM$ (1:4.5) achieved the best performance with a PCE of 5.73%, together with a V_{oc} of 1.02 V, a J_{sc} of 10.75 mA cm^{-2} and an improved FF of 52.22%.

The J-V curves and the EQE spectra for **P3FTBT1**, **P3FTBT1F**, and **P3FTBT8O6** are plotted in Fig. 5. The photovoltaic parameters (V_{oc}, J_{sc}, FF and PCE) are summarized in Table 2. **P3FTBT1** was designed and obtained by replacing the two central hexyl chains on **P3FTBT6** (Scheme 1) with the smallest alkyl groups (methyl). Compared to the **P3FTBT6**-based solar cell, the FF of **P3FTBT1**-based device increases significantly from 44% to 51.65%, leading to an enhanced PCE of 5.39%. **P3FTBT1F** and **P3FTBT1O6** were designed by incorporating F atoms or hexyoxy groups into the **BT** unit, respectively. A PCE of 5.73% with a V_{oc} above 1.0 V was achieved for **P3FTBT1O6**-based solar cells. And the PSC fabricated from **P3FTBT1F** exhibits a PCE of 4.50% with a V_{oc} up to 1.09 V (Table S4†), which agrees with its deep-lying HOMO energy level. Whereas, the best performance device based on **P3FTBT1F** exhibits a PCE of 4.60 % with a V_{oc} of 1.08 V (Table S4†). However, when the two hexyl chains were changed to the bulky 2-ethylhexyl chains, **P3FTBT8O6** exhibits a low average PCE of 2.60% with a V_{oc} of 1.03 V, an FF of 34.99% and a low J_{sc} of 7.24 mA/cm^2. In comparison with **P3FTBT1O6**, the performance of PSCs based on **P3FTBT8O6** declined sharply, due to bulky side chains which are not favourable for a good π-π packing. It is also supported by the lower hole mobilities obtained from both OFET and hole-only devices. It is worth noting that too many short alkyl chains may lead to poor solubility of the resulting copolymers. Therefore the other four hexyl chains are not changed to ensure that these polymers can be easily dissolved in common organic solvents. It is noted that the molecular weights of **P3FTBT8O6** is relatively smaller compared to the other three copolymers which may be an additional factor responsible for its inferior device performance besides the side-chain difference.

Table 2 Device parameters of PSCs based on different copolymers

Polymers	D:A[a]	V_{oc} (V)	J_{sc} (mA/cm^2)	FF (%)	PCE (%)	R_{sh}[c] (kΩ cm^2)	R_s[c] (Ω cm^2)	Refs
		Max. (Avg.[b])	Max. (Avg.[b])	Max. (Avg.[b])	Max. (Avg.[b])			
P3FTBT6	1:4.0	1.04	10.3	0.42	/	/	/	Ref 4
P3FTBT1	1:4.5	1.02 (1.02 ± 0.01)	10.21 (9.77 ± 0.47)	51.65 (51.02 ± 0.87)	5.39 (5.10 ± 0.29)	0.53	13.7	this work
P3FTBT1F	1:4.5	1.08 (1.08 ± 0.01)	9.16 (8.81 ± 0.49)	46.65 (47.06 ± 1.52)	4.60 (4.47 ± 0.18)	0.45	21.8	this work
P3FTBT8O6	1:4.5	1.04 (1.03 ± 0.02)	7.72 (7.24 ± 1.19)	35.57 (34.99 ± 4.30)	2.86 (2.60 ± 0.26)	0.35	47.3	this work
P3FTBT1O6	1:3.0	1.02 (1.02 ± 0.01)	9.41 (9.41 ± 0.19)	46.42 (45.52 ± 1.21)	4.47 (4.39 ± 0.10)	0.30	18.3	this work
P3FTBT1O6	1:4.0	1.00 (1.01 ± 0.02)	10.91 (10.23 ± 0.68)	47.83 (48.43 ± 0.77)	5.24 (5.00 ± 0.24)	0.40	14.4	this work
P3FTBT1O6	1:4.5	1.02 (1.01 ± 0.01)	10.75 (10.54 ± 0.22)	52.22 (52.40 ± 0.73)	5.73 (5.61 ± 0.12)	0.55	13.6	this work
P3FTBT1O6	1:5.0	1.01 (1.01 ± 0.01)	10.05 (9.70 ± 0.34)	52.00 (52.50 ± 1.09)	5.29 (5.15 ± 0.14)	0.61	13.9	this work

[a]Blend ratios of polymer:$PC_{71}BM$ (w/w). [b]The average values were obtained from eight devices. [c]The R_s and R_{sh} values were obtained from the highest PCE device.

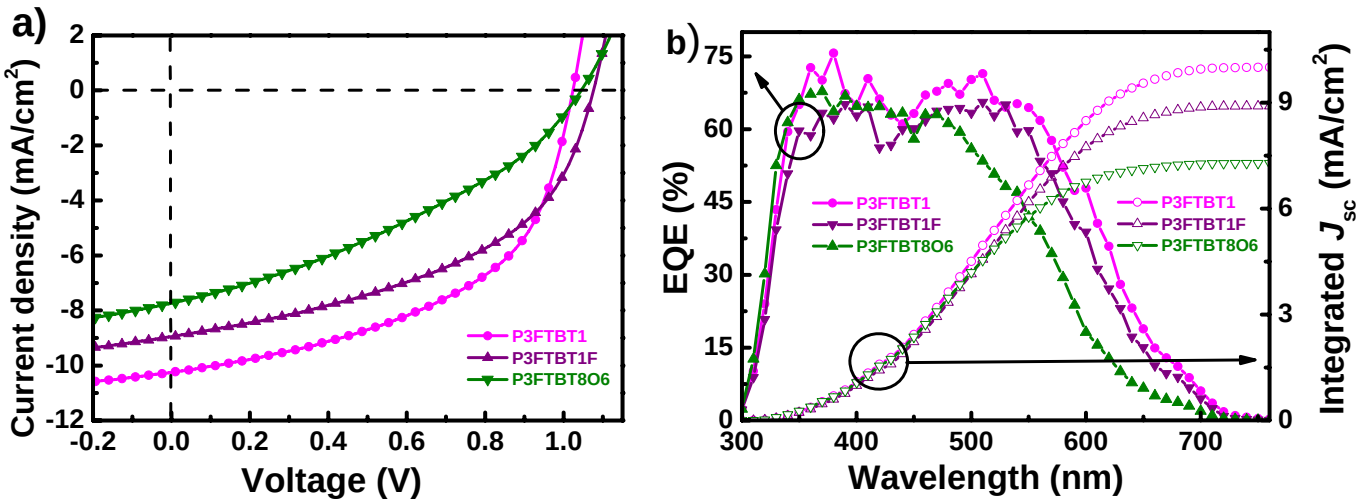

Fig. 5 a) *J*–*V* curves and b) EQE and corresponding integrated J_{sc} curves of PSCs based on polymers blended with $PC_{71}BM$.

External Quantum Efficiency

The EQE curves of PSCs based on **P3FTBT1O6** blended with $PC_{71}BM$ with various blend ratios and the other three polymers blended with $PC_{71}BM$ with a blend ratio of 1:4.5 are plotted in Figs. 3b and 5b, respectively. All PSCs show a photon response in the wavelength range from 300 to 700 nm which is in agreement with the UV-vis absorption spectra of the polymer:$PC_{71}BM$ blend films. As shown in Fig. 3b, in the whole photon response range, the EQE values of the devices fabricated from **P3FTBT1O6**:$PC_{71}BM$ (1:4.5, w/w) is higher than that of others. The EQE values for the **P3FTBT8O6**-based devices decrease sharply compared to other three polymer-based devices which agrees with their low J_{sc} values. Integrating the EQE data with the AM 1.5G spectrum gave calculated J_{sc} values of ~9.47, 10.40, 10.60 and 9.83 mA cm^{-2} for the PSCs based on the **P3FTBT1O6**:$PC_{71}BM$ with various blend ratios (D:A = 1:3.0, 1:4.0, 1:4.5 and 1:5.0), respectively (Fig. 3b). These values are in well agreement with the measured J_{sc} values in Fig. 3a. The calculated J_{sc} values of PSCs based on **P3FTBT1**, **P3FTBT1F**, **P3FTBT8O6** are ~10.01, 8.90, and 7.29 mA cm^{-2}, respectively (Fig. 5b), and they also match well with the measured J_{sc} values in Fig. 5a.

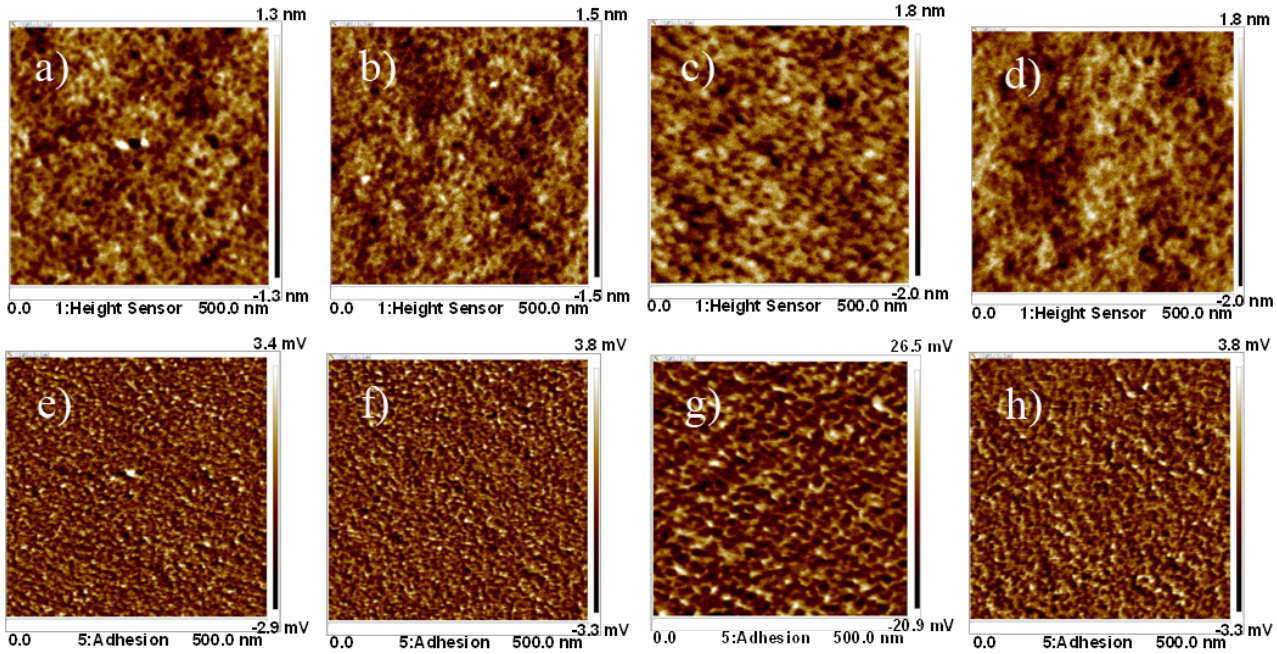

Fig. 6 AFM topography (top) and phase (bottom) images of blend films spin-coated from **P3FTBT1O6**:$PC_{71}BM$ with different blend ratios: (a, e) **P3FTBT1O6**:$PC_{71}BM$ = 1:3.0, (b, f) **P3FTBT1O6**:$PC_{71}BM$ = 1:4.0, (c, g) **P3FTBT1O6**:$PC_{71}BM$ = 1:4.5, (d, h) **P3FTBT1O6**:$PC_{71}BM$ = 1:5.0.

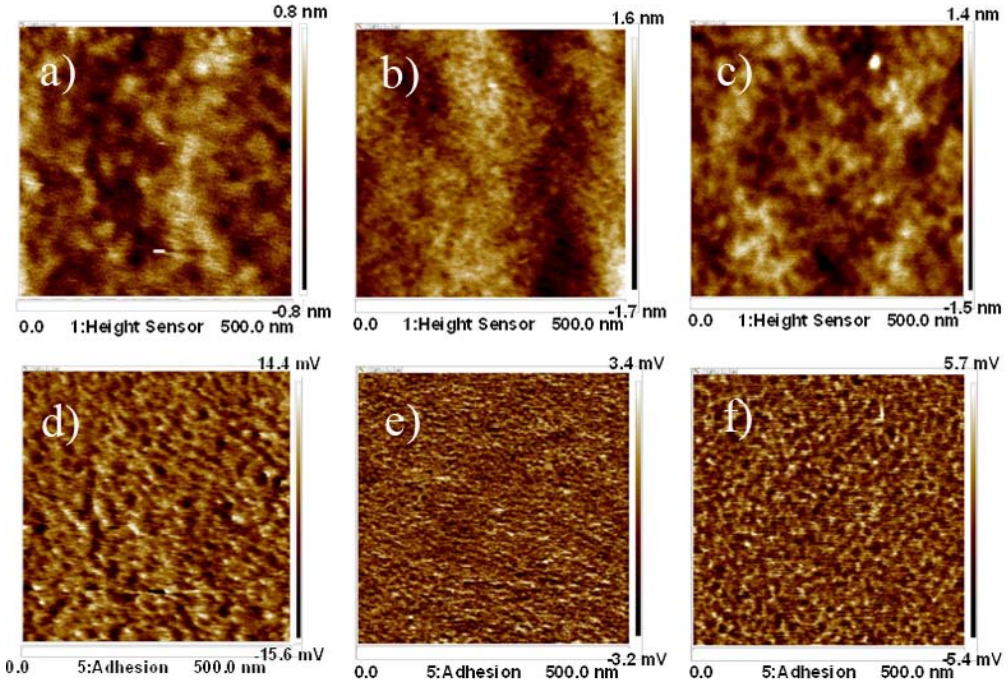

Fig. 7 AFM topography (top) and phase (bottom) images of blend films spin-coated from polymer:$PC_{71}BM$ (1:4.5, w/w) solution: (a, d) **P3FTBT1**:$PC_{71}BM$, (b, e) **P3FTBT1F**:$PC_{71}BM$, (c, f) **P3FTBT8O6**:$PC_{71}BM$.

Morphology

Nanoscale phase separation is required for the active layer in high performance PSCs, and it will enable a large interface area for exciton dissociation and, at the same time, a continuous percolating path for electron and hole transport to the corresponding electrodes.[45] Therefore, tapping mode AFM were performed to investigate the surface morphology of the BHJ blend films and the results are shown in Figs. 6 and 7. Although the images for all the polymer blends show relatively flat surfaces and clear phase separation features, the domain size and phase separation feature of these blend films are affected by the fullerene:polymer blend ratio as well as the side chains of the polymers. Fig. 6 shows topography and phase AFM images of **P3FTBT1O6**:$PC_{71}BM$ films cast with increasing amounts of $PC_{71}BM$. The results demonstrate that the phase separation and domain size are sensitive to the blend ratio of **P3FTBT1O6** to $PC_{71}BM$. As the ratio of $PC_{71}BM$ to **P3FTBT1O6** progressively increases from 3.0:1, to 4.0:1, and to 4.5:1, the nanoscale phase separation can be seen more clearly. However, when the ratio further increases to 5.0:1, the phase separation becomes less clear compared to that for the film with the 4.5:1 ratio. The most pronounced phase separation with an optimal domain size of ~10-20 nm for the **P3FTBT1O6**:$PC_{71}BM$ film (1:4.5) is responsible for the highest PCE for the corresponding device as discussed in the previous section. Further, The morphology of the **P3FTBT1O6**:$PC_{71}BM$ (1:4.5) blend film was also studied by transmission electron microscopy (TEM), and the result is shown in Fig. S6†. The higher electron density of $PC_{71}BM$ compared with **P3FTBT1O6** causes electrons to be scattered more efficiently by the $PC_{71}BM$ from the TEM beam.[46] Thus, the dark regions in Fig. S6 are attributed as $PC_{71}BM$ clusters, whereas the bright regions are assigned to **P3FTBT1O6**. The morphology of the blend film is generally uniform and there is no large phase separation. These TEM results reconfirm the nanoscale phase separation (~10-20 nm) for the **P3FTBT1O6**:$PC_{71}BM$ layer. From Figs. 6 & 7, it is found that the domain size of the BHJ film is also dependent on the structure of the polymers. For example, strong nanoscale phase separation with domain sizes of around 10-20 nm can be found for the polymer blends based on **P3FTBT1** and **P3FTBT1O6**, which is in favor of the high J_{sc} values of their corresponding solar cells. However, the phase separation for polymer blends based on **P3FTBT1F** and **P3FTBT8O6** is less pronounced compared to that for the other two polymer blends, which contributes to the reduced PCEs for the corresponding devices.

It is found that **P3FTBT1O6**:$PC_{71}BM$ blend films with different blend ratios (D:A = 1:3.0, 1:4.0, 1:4.5 and 1:5.0) have root-mean-square (r.m.s.) surface roughnesses of 0.369, 0.426, 0.546 and 0.543 nm, respectively. The AFM measurements indicate the influence of blend ratio on the surface morphology of the active layers. The roughnesses of **P3FTBT1**:$PC_{71}BM$ (1:4.5), **P3FTBT1F**:$PC_{71}BM$ (1:4.5), **P3FTBT8O6**:$PC_{71}BM$ (1:4.5) and **P3FTBT1O6**:$PC_{71}BM$ (1:4.5) are 0.233, 0.509, 0.419 and 0.546 nm, respectively. The polymer blend film based on **P3FTBT1** has the smoothest surface which is reasonable considering the least bulky side chains in the polymer backbone. And the polymer blend film based on **P3FTBT8O6** has the roughest surface due to the most bulky alkyl chains. The results demonstrate that the morphology of polymer blends is closely related to the side chains used for the copolymers.

Conclusions

A series of ladder-type tetra-*p*-phenylene containing copolymers **P3FTBT1**, **P3FTBT1F**, **P3FTBT8O6** and **P3FTBT1O6** were designed, synthesized by side-chain tailoring. **P3FTBT1O6** exhibits the highest PCE of 5.73% while combining a FF of 52.2% and a V_{oc} of 1.02 V. However, the PCE of the **P3FTBT8O6**-based device declines sharply to

2.86%. The **P3FTBT1F**-based device shows a PCE of 4.50% with a high V_{oc} of 1.09 V. These results indicate that the shortest methyl groups of the ladder-type tetra-*p*-phenylene unit may contribute to better morphology, a higher mobility as well as a higher PCE than the hexyl or 2-ethylhexyl substituted counterparts. The incorporation of F atoms into the **BT** unit afforded copolymers with a deeper-lying HOMO energy level and a high V_{oc} of 1.09 V for the resulting PSCs. The introduction of hexyloxy groups to the **BT** unit leads to **P3FTBT1O6** with the best device performance. The results demonstrate that the ladder-type tetra-*p*-phenylene containing copolymers are promising candidates for high efficiency PSCs with high V_{oc}s. At the same time, these large band-gap (~2.0 eV) copolymers can be used as short-wavelength absorbing materials for tandem solar cells with high V_{oc}s.

Acknowledgements

This work was supported by the National Natural Science Foundation of China (Nos. 61325026, 51173186 and 51203158), the Natural Science Foundation of Fujian Province (No. 2014J01216), and the CAS/SAFEA International Partnership Program for Creative Research Teams.

Notes and references

[a]State Key Laboratory of Structural Chemistry, Fujian Institute of Research on the Structure of Matter, Chinese Academy of Sciences, Fuzhou, 350002, P. R. China *E-mail: qingdongzheng@fjirsm.ac.cn; Fax: (+)86-591-63173282
[b]University of Chinese Academy of Sciences, Beijing 100049, P.R. China

† Electronic Supplementary Information (ESI) available: Figures showing the absorption spectra of the blended films, the transfer curves (in air) of OFETs based on polymers, the $J^{0.5}$-V characteristics of hole-only devices based on the polymers and the $J^{0.5}$-V characteristics of hole-only devices based on **P3FTBT1O6**:$PC_{71}BM$ with different blend ratios, device parameters of PSCs, TEM image of the **P3FTBT1O6**:$PC_{71}BM$ blend film, synthetic details for the copolymers, and NMR spectra of new monomers. See DOI: 10.1039/b000000x

1. Z. He, C. Zhong, S. Su, M. Xu, H. Wu and Y. Cao, *Nat Photon*, 2012, **6**, 591-595.
2. B. Kan, Q. Zhang, M. Li, X. Wan, W. Ni, G. Long, Y. Wang, X. Yang, H. Feng and Y. Chen, *J. Am. Chem. Soc.*, 2014, **136**, 15529-15532.
3. J. You, L. Dou, K. Yoshimura, T. Kato, K. Ohya, T. Moriarty, K. Emery, C.-C. Chen, J. Gao, G. Li and Y. Yang, *Nat Commun*, 2013, **4**, 1446.
4. Q. Zheng, B. Jung, J. Sun and H. E. Katz, *J. Am. Chem. Soc.*, 2010, **132**, 5394-5404.
5. C. Cui, W.-Y. Wong and Y. Li, *Energy Environ. Sci.*, 2014, **7**, 2276-2284.
6. E. T. Hoke, K. Vandewal, J. A. Bartelt, W. R. Mateker, J. D. Douglas, R. Noriega, K. R. Graham, J. M. J. Fréchet, A. Salleo and M. D. McGehee, *Adv. Energy Mater.*, 2013, **3**, 220-230.
7. C. Liu, C. Yi, K. Wang, Y. Yang, R. S. Bhatta, M. Tsige, S. Xiao and X. Gong, *ACS Appl. Mater. Interfaces*, 2015, **7**, 4928-4935.
8. Y. Liu, J. Zhao, Z. Li, C. Mu, W. Ma, H. Hu, K. Jiang, H. Lin, H. Ade and H. Yan, *Nat. Commun.*, 2014, **5**, 5293.
9. H. Zhou, Y. Zhang, C.-K. Mai, S. D. Collins, G. C. Bazan, T.-Q. Nguyen and A. J. Heeger, *Adv. Mater.*, 2015, **27**, 1767-1773.
10. J.-M. Jiang, P.-A. Yang, S.-C. Lan, C.-M. Yu and K.-H. Wei, *Polymer*, 2013, **54**, 155-161.
11. S.-C. Chen, C. Tang, Z. Yin, Y. Ma, D. Cai, D. Ganeshan and Q. Zheng, *Chin. J. Chem.*, 2013, **31**, 1409-1417.
12. H. Li, S. Sun, S. Mhaisalkar, M. T. Zin, Y. M. Lam and A. C. Grimsdale, *J. Mater. Chem. A*, 2014, **2**, 17925-17933.
13. J. C. Bijleveld, R. A. M. Verstrijden, M. M. Wienk and R. A. J. Janssen, *Appl. Phys. Lett.*, 2010, **97**, 073304.
14. J. Warnan, C. Cabanetos, R. Bude, A. El Labban, L. Li and P. M. Beaujuge, *Chem. Mater.*, 2014, **26**, 2829-2835.
15. J. Cremer, P. Bäuerle, M. M. Wienk and R. A. J. Janssen, *Chem. Mater.*, 2006, **18**, 5832-5834.
16. A. Casey, R. S. Ashraf, Z. P. Fei and M. Heeney, *Macromolecules*, 2014, **47**, 2279-2288.
17. J. Huang, Y. Zhao, W. He, H. Jia, Z. Lu, B. Jiang, C. Zhan, Q. Pei, Y. Liu and J. Yao, *Polym. Chem.*, 2012, **3**, 2832-2841.
18. J. Huang, X. Wang, C. Zhan, Y. Zhao, Y. Sun, Q. Pei, Y. Liu and J. Yao, *Polym. Chem.*, 2013, **4**, 2174-2182.
19. C. Cabanetos, A. El Labban, J. A. Bartelt, J. D. Douglas, W. R. Mateker, J. M. J. Fréchet, M. D. McGehee and P. M. Beaujuge, *J. Am. Chem. Soc.*, 2013, **135**, 4656-4659.
20. C. Piliego, T. W. Holcombe, J. D. Douglas, C. H. Woo, P. M. Beaujuge and J. M. J. Fréchet, *J. Am. Chem. Soc.*, 2010, **132**, 7595-7597.
21. X. Xu, Y. Wu, J. Fang, Z. Li, Z. Wang, Y. Li and Q. Peng, *Chem. Eur. J.*, 2014, **20**, 13259-13271.
22. L. Wang, D. Cai, Z. Yin, C. Tang, S.-C. Chen and Q. Zheng, *Polym. Chem.*, 2014, **5**, 6847-6856.
23. P. M. Beaujuge, H. N. Tsao, M. R. Hansen, C. M. Amb, C. Risko, J. Subbiah, K. R. Choudhury, A. Mavrinskiy, W. Pisula, J. L. Brédas, F. So, K. Müllen and J. R. Reynolds, *J. Am. Chem. Soc.*, 2012, **134**, 8944-8957.
24. P. M. Beaujuge, W. Pisula, H. N. Tsao, S. Ellinger, K. Müllen and J. R. Reynolds, *J. Am. Chem. Soc.*, 2009, **131**, 7514-7515.
25. Q. Liu, C. Li, E. Jin, Z. Lu, Y. Chen, F. Li and Z. Bo, *ACS Appl. Mater. Interfaces*, 2014, **6**, 1601-1607.
26. B. Liu, X. Chen, Y. Zou, L. Xiao, X. Xu, Y. He, L. Li and Y. Li, *Macromolecules*, 2012, **45**, 6898-6905.
27. J. Lee, S. B. Jo, M. Kim, H. G. Kim, J. Shin, H. Kim and K. Cho, Adv. Mater., 2014, 26, 6706–6714.
28. Y. Ma, Q. Zheng, L. Wang, D. Cai, C. Tang, M. Wang, Z. Yin and S.-C. Chen, *J. Mater. Chem. A*, 2014, **2**, 13905-13915.
29. H. Zhou, L. Yang, A. C. Stuart, S. C. Price, S. Liu and W. You, *Angew. Chem. Int. Ed.*, 2011, **50**, 2995-2998.
30. Z. Li, J. Lu, S.-C. Tse, J. Zhou, X. Du, Y. Tao and J. Ding, *J. Mater. Chem.*, 2011, **21**, 3226-3233.
31. J.-F. Jheng, Y.-Y. Lai, J.-S. Wu, Y.-H. Chao, C.-L. Wang and C.-S. Hsu, *Adv. Mater.*, 2013, **25**, 2445-2451.
32. B. C. Schroeder, R. Ashraf, S. Thomas, A. J. P. White, L. Biniek, C. Nielsen, W. Zhang, Z. Huang, P. S. Tuladhar and S. E. Watkins, *Chem. Commun.*, 2012, **48**, 7699-7701.
33. J. Min, Z.-G. Zhang, S. Zhang and Y. Li, *Chem. Mater.*, 2012, **24**, 3247-3254.

34. T. L. Nguyen, H. Choi, S.-J. Ko, M. A. Uddin, B. Walker, S. Yum, J.-E. Jeong, M. H. Yun, T. Shin and S. Hwang, *Energy Environ. Sci.*, 2014, **7**, 3033-3039.
35. J. W. Jo, S. Bae, F. Liu, T. P. Russell and W. H. Jo, *Adv. Funct. Mater.*, 2014, **25**, 120-125.
36. Q. Zheng, S. K. Gupta, G. S. He, L.-S. Tan and P. N. Prasad, *Adv. Funct. Mater.*, 2008, **18**, 2770-2779.
37. R. D. Hreha, C. P. George, A. Haldi, B. Domercq, M. Malagoli, S. Barlow, J. L. Brédas, B. Kippelen and S. R. Marder, *Adv. Funct. Mater*., 2003, **13**, 967-973.
38. B. Fu, J. Baltazar, Z. Hu, A.-T. Chien, S. Kumar, C. L. Henderson, D. M. Collard and E. Reichmanis, *Chem. Mater.*, 2012, **24**, 4123-4133.
39. M. Helgesen, S. A. Gevorgyan, F. C. Krebs and R. A. Janssen, *Chem. Mater.*, 2009, **21**, 4669-4675.
40. Y. Ma, Q. Zheng, Z. Yin, D. Cai, S.-C. Chen and C. Tang, *Macromolecules*, 2013. **46**, 4813-4821.
41. N. Blouin, A. Michaud, D. Gendron, S. Wakim, E. Blair, R. Neagu-Plesu, M. Belletête, G. Durocher, Y. Tao and M. Leclerc, *J. Am. Chem. Soc.*, 2007, **130**, 732-742.
42. Q. Peng, K. Park, T. Lin, M. Durstock and L. Dai, *J. Phys. Chem. B*, 2008, **112**, 2801-2808.
43. J. D. Servaites, M. A. Ratner and T. J. Marks, *Energy Environ. Sci.*, 2011, **4**, 4410-4422.
44. R. Steyrleuthner, M. Schubert, F. Jaiser, J. C. Blakesley, Z. Chen, A. Facchetti and D. Neher, *Adv. Mater.*, 2010, **22**, 2799-2803.
45. W. Li, K. H. Hendriks, A. Furlan, W. S. C. Roelofs, S. C. J. Meskers, M. M. Wienk and R. A. J. Janssen, *Adv. Mater.*, 2013, **26**, 1565-1570
46. S. H. Park, A. Roy, S. Beaupre, S. Cho, N. Coates, J. S. Moon, D. Moses, M. Leclerc, K. Lee and A. J. Heeger, *Nat. Photonics*, 2009, **3**, 297-302.

A table of contents entry

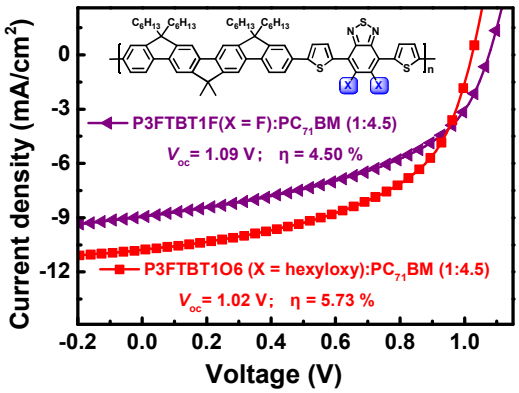

Side-chain engineering on the polymer backbone of ladder-type tetra-*p*-phenylene-based copolymers leads to polymer solar cells with high open circuit voltages.